Supporting Information for: Dilute suspensions of Janus rods: the role of bond and shape anisotropy

Carlo Andrea De Filippo, Sara Del Galdo, Emanuela Bianchi, Cristiano De Michele, and Barbara Capone

1 Aggregation-Volume-Bias

The Aggregation Volume Bias Monte Carlo (AVB-MC) algorithm is designed to improve the phase space sampling of cluster forming systems. AVB-MC enhances the acceptance rate of trial moves that result in molecular clusters breaking up, and simultaneously increases the transition probability of moves that lead to the formation of bonded structures [1, 2, 3]. In this work the AVB-MC algorithm is designed so that the system has a 90% probability of making either a translation or a rotation move, where both moves are chosen to have equal probability. To improve the phase space sampling, we introduce a biased move with a probability of 10%, which can be either a bonding (AVB-B) or an unbonding (AVB-U) trial move with equal probability. The AVB-B move is designed to form a bond between two unbounded particles, while the AVB-U move is designed to break an existing bond. The standard AVB-MC algorithm, makes use of the bonding volume V_b – defined as the portion of the phase-space in which two particles are bonded – to weight both AVB-B and AVB-U moves within the metropolis algorithm. In the case of two particles of diameter D decorated with a Kernel-Frenkel patch of $\delta/2$ range and of θ half opening, the bonding volume can be computed analytically as:

$$V_b = \frac{4\pi^2}{3}(1-\cos\theta)^2\left((D+\delta)^3 - D^3\right) \tag{1}$$

Let us introduce the concept of outer volume V_o, defined as the number of non-bonding configurations in the phase space:

$$V_o = 4\pi V - V_b \tag{2}$$

where V is the volume of the simulation box and 4π comes from the orientational degrees of freedom. Given a system of N_p patches, where N_i is the number of patches bound to the p_i patch of the i-th particle, then within the AVB-MC scheme:

1. in the case of the AVB-B move, the trial is accepted with probability

$$acc(o \to n) = min\left\{1, \frac{(N_p - N_i - 1)V_b}{(N_i + 1)V_o} e^{-\beta \Delta \mathcal{U}}\right\} \tag{3}$$

   where $\Delta \mathcal{U}$ is the energy difference between the two configurations

2. while in the case of AVB-U move, the acceptance probability is

$$acc(o \to n) = min\left\{1, \frac{N_i V_o}{(N_p - N_i)V_b} e^{-\beta \Delta \mathcal{U}}\right\} \tag{4}$$

AVB-MC algorithm has been used so far in literature to enhance the sampling in the case of cluster forming spherical particles. In this work, the algorithm is generalised to the case of elongated rods; this requires that, once the patch is moved into a bonded/unbonded configuration, the body of the elongated particle has to be rototranslated to rebuild the original symmetry of the particle.

2 Phase diagram as a function of ρ

In Figure 1 we report the phase diagram of the system as a function of the density $\rho = N/V$. It is possible to appreciate that the cmc for fixed (δ, ε) is reached almost at the same density for all the elongations A. This is due to the fact that the emergence of clustering only depends on the tip-tip interactions, that is the effective density of patches.

3 Literature comparison

We compared the average number of bonds per particles as a function of ϕ and ε that we obtained for Janus spheres ($A = 0$) with interaction range $\delta/2 = 0.25$ with available data from literature (Sciortino *et al.* [4, 5]). The comparison is reported in Fig. 2, which shows the very good agreement between the two data sets.

4 Analysis of intra-cluster arrangement

The three order parameters used in this work ($\mathcal{M}$, $\mathcal{V}$, and $\mathcal{B}$) describe the overall structure of the cluster. To have a more in-depth understanding of what differentiates the different cluster structures at fixed state points in the phase diagram, we set our attention on the relative orientations between all the bonded couples of particles. To this aim, we computed the distribution of scalar products $P(\hat{n}_i \cdot \hat{n}_j)$, where $\hat{n}_i$ and $\hat{n}_j$ are the unit vectors describing the orientation of particles i and j. Moreover, we obtained the average number of bonds per particle.

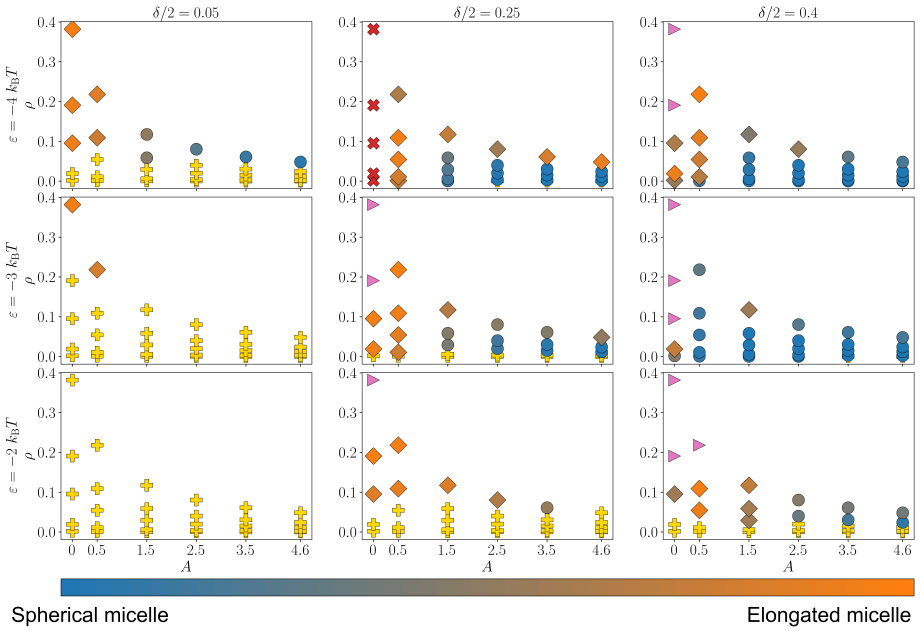

Figure 1: Phase diagram as a function of A, δ, ε and $\rho = N/V$ reporting the most probable cluster phase for every state point. The marker type represents the dominant cluster phase: systems below cmc (yellow plus symbols), vesicles (red crosses), extended clusters (pink triangles), spherical micelles (circles), and elongated micelles (diamonds). About micelles, to highlight the coexistence of spherical and elongated structures, the corresponding marker colour reflects the cluster type probability, spanning from blue for predominantly spherical micelles to orange for predominating elongated ones.

In Fig. 3 we analysed the extended clusters emerging from systems with $\delta/2 = 0.4$, $A = 0$, and $\phi = 0.2$ as a function of ε. It is clear that for $\varepsilon = -2k_{\mathrm{B}}T$ the particles arrange into a disordered liquid-like structure. The ordering increases with ε, leading to a concurrent increase in the number of bonds.

The nature of the elongated micelles emerging in the systems with $\delta/2 = 0.25$, $A = 0.5$, and $\phi = 0.1$ as a function of ε is analysed in Fig. 4. With ε the internal order of the structures increases, which is mirrored both by an increase in the average number of bonds and by a transition from a disordered structure ($\varepsilon = -2k_{\mathrm{B}}T$) to a more ordered one ($\varepsilon = -4k_{\mathrm{B}}T$).

Finally, we analysed the apparent reentrant behaviour as a function of ε that is observed for systems with $\delta/2 = 0.4$, $A = 0.5$, and $\phi = 0.1$. In fact, for this system, upon augmenting the interaction strength ε, the most stable phases are elongated micelles for $\varepsilon = -2k_{\mathrm{B}}T$, spherical micelles for $\varepsilon = -3k_{\mathrm{B}}T$, and again elongated micelles for $\varepsilon = -4k_{\mathrm{B}}T$. To understand such a feature, we can focus on the local arrangement of particles in the different clusters, in terms of the

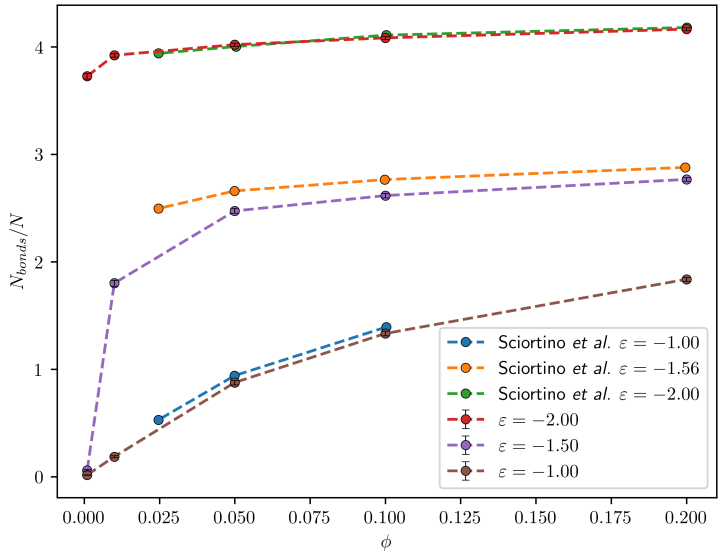

Figure 2: Average number of bonds per particle for Janus spheres ($A = 0$) as a function of ϕ and ε for systems with $\delta/2 = 0.25$. Data from Sciortino *et al.* [4, 5] (blue, orange and green symbols) are reported along with our data (red, purple and brown symbols) for comparisons.

relative orientation of particles. Through the combination of the distributions $P(\hat{n}_i \cdot \hat{n}_j)$ and the average number of bonds per particle, it emerges that:

- in the case of $\varepsilon = -2k_{\mathrm{B}}T$ the particles arrange into a liquid-like structure;
- for $\varepsilon = -3k_{\mathrm{B}}T$ the spherical nature of the clusters emerges;
- for $\varepsilon = -4k_{\mathrm{B}}T$ the particles form elongated clusters, locally resembling bilayers and/or long tubes.

This indicates that, even if the system apparently stabilises twice elongated clusters, the intrinsic nature of the aggregate is different. For the lowest value of ε elongated clusters are disordered, differently than the ones assembled at the highest value of ε that, arising form the merging of spherical micelles, present a local order between the colloidal particles.

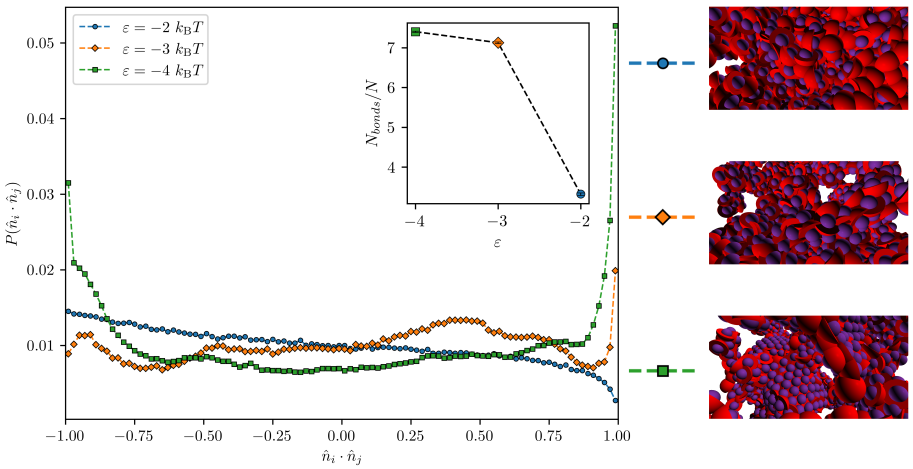

Figure 3: Distribution of the scalar product $\hat{n}_i \cdot \hat{n}_j$ evaluated over all pairs of bonded particles for the system with $\delta/2 = 0.4$, $A = 0$, and $\phi = 0.2$ as a function of ε. In the inset the average number of bonds per particle is reported. Representative snapshots of the three types of extended clusters analysed are also included.

References

[1] Bin Chen and J. Ilja Siepmann. A novel monte carlo algorithm for simulating strongly associating fluids: applications to water, hydrogen fluoride, and acetic acid. The Journal of Physical Chemistry B, 104(36):8725–8734, 2000.

[2] Bin Chen, J. Ilja Siepmann, Kwang J. Oh, and Michael L. Klein. Aggregation-volume-bias Monte Carlo simulations of vapor-liquid nucleation barriers for Lennard-Jonesium. The Journal of Chemical Physics, 115(23):10903–10913, 12 2001.

[3] Bin Chen and J. Ilja Siepmann. Improving the efficiency of the aggregation-volumebias monte carlo algorithm. The Journal of Physical Chemistry B, 105(45):11275–11282, 2001.

[4] Francesco Sciortino, Achille Giacometti, and Giorgio Pastore. Phase diagram of janus particles. Phys. Rev. Lett., 103:237801, Nov 2009.

[5] Francesco Sciortino, Achille Giacometti, and Giorgio Pastore. A numerical study of one-patch colloidal particles: from square-well to janus. Phys. Chem. Chem. Phys., 12:11869–11877, 2010.

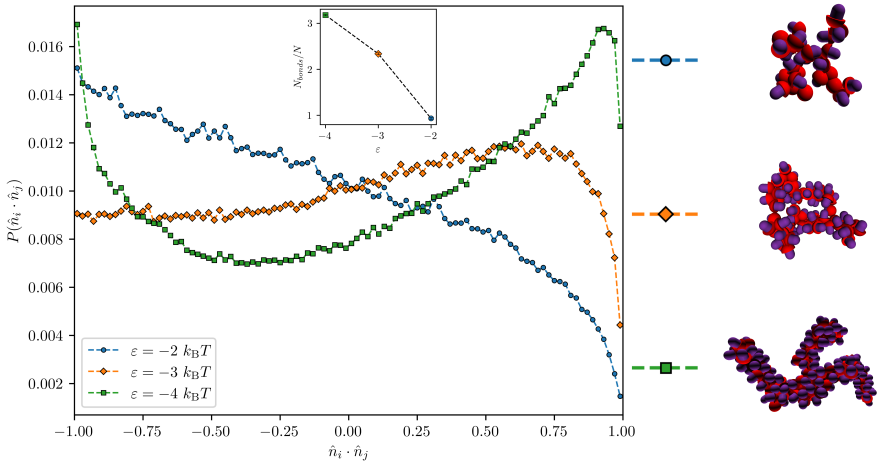

Figure 4: Distribution of the scalar product $\hat{n}_i \cdot \hat{n}_j$ evaluated over all pairs of bonded particles for the system with $\delta/2 = 0.25$, $A = 0.5$, and $\phi = 0.1$ as a function of ε. In the inset the average number of bonds per particle is reported. Representative snapshots of the cluster with the maximum size observed in the systems analysed are also included.

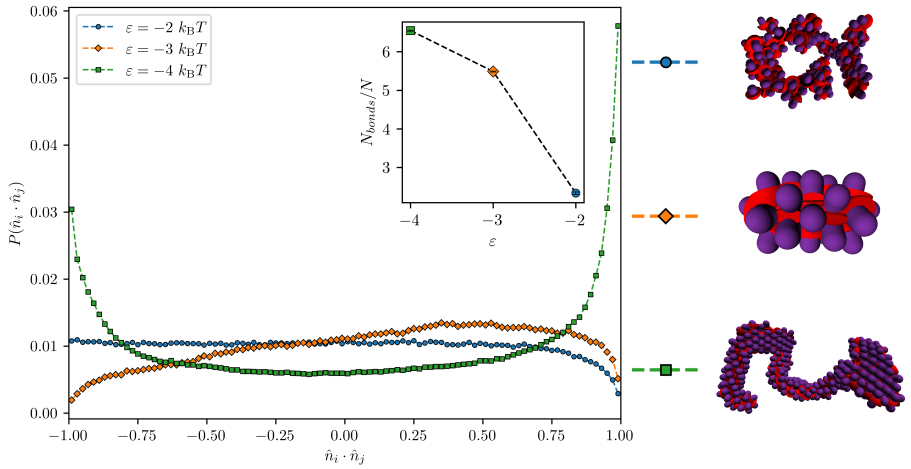

Figure 5: Distribution of the scalar product $\hat{n}_i \cdot \hat{n}_j$ evaluated over all pairs of bonded particles for the system with $\delta/2 = 0.4$, $A = 0.5$, and $\phi = 0.1$ as a function of ε. In the inset the average number of bonds per particle is reported. Representative snapshots of the cluster with the maximum size observed in the systems analysed are also included.